Magnetic Order in $Nd_{2-x}Ce_xCuO_{4-\delta}$

Matthew J. Rosseinsky,*[a] Kosmas Prassides,*[b] and Peter Day[c]

[a] *Inorganic Chemistry Laboratory, Oxford University, Oxford OX1 3QR, U.K.*
[b] *School of Chemistry and Molecular Sciences, Sussex University, Brighton BN1 9QJ, U.K.*
[c] *Institut Laue-Langevin, 38042 Grenoble Cedex, France*

The magnetic structures of Nd_2CuO_4 and $Nd_{1.97}Ce_{0.03}CuO_4$ have been solved at 1.6 K using powder neutron diffraction methods, and the magnetic cell (magnetic space group *C'mm'm'*) results from a $\sqrt{2} \times \sqrt{2}$ rotation of the basal plane of the *I4/mmm* nuclear unit cell, with a Cu spin direction $(\frac{1}{2},\frac{1}{2},0)$ parallel to the magnetic propagation vector $\boldsymbol{k} = (\frac{1}{2},\frac{1}{2},0)$; the Nd spins are also constrained by symmetry to lie in the same direction, while the Néel state is not very sensitive to electron doping in contrast to the extreme sensitivity to hole doping of the Néel state in La_2CuO_4, and a lower limit for the Cu ordering temperature is estimated to be 170 K.

The discovery of superconductivity in copper oxide systems[1] has led to intensive theoretical and experimental study of their electronic and magnetic structures. Even the apparently simple alkaline earth doped derivatives of La_2CuO_4 display a remarkably rich structural and magnetic phase diagram.[2] The role of strong electronic correlations is central to the understanding of the physics of the high-T_c materials together with the intimate relation between the magnetic and (super)-conducting properties of the CuO_2 layers. Recently, it has been demonstrated that electron doping of Ln_2CuO_4 (Ln ≠ La) also leads to superconducting compositions,[3] $Ln_{2-x}Ce_x$-CuO_4.Ln_2CuO_4[4] (*e.g.* Ln = Nd) differs structurally from La_2CuO_4 in that the co-ordination number of Cu is reduced to 4, with no bridging oxygen between Ln and Cu along the *c*-axis and an expanded basal plane. This leads to band narrowing and further increases the importance of correlations. Luke *et al.*[5] have studied the magnetic properties of these phases using muon spin rotation measurements and established the existence of magnetic order on the μSR timescale below 300 K. There is also possible interaction of the copper with the rare-earth spin sublattice, a feature not present in La_2CuO_4 and its hole-doped derivatives. The magnetic structure determination for Ln_2CuO_4 and its electron-doped derivatives is thus crucial to the understanding of the competition between magnetism and superconductivity in any model for the high-T_c compounds.

Nd_2CuO_4 was synthesised by the citrate sol–gel technique[6,7] and $Nd_{1.97}Ce_{0.03}CuO_4$ by standard solid-state reactions.[3,7] Powder neutron diffraction measurements were performed using the high intensity D1B diffractometer at ILL, Grenoble, between 1.6 and 320 K at λ = 2.52 Å using a pyrolytic graphite monochromator. Subtraction of 50 K and 5 K data from 1.6 K data revealed the presence of seven magnetic peaks which could be indexed on the basis of a $\sqrt{2} \times \sqrt{2}$ rotation of the basal plane of the *I4/mmm* unit cell, corresponding to the X point $(\frac{1}{2},\frac{1}{2},0)$ of the body-centred tetragonal Brillouin zone, with the point group of the wave vector $G(\boldsymbol{k})$ as $D_{2h}(mmm)$. We then performed a representation analysis of magnetic structure[8] by constructing transformation matrices *T*, forming a unitary multiplier representation of $G(\boldsymbol{k})$. Irreducible representations spanned by the basis functions constructed from magnetic moments at Nd and Cu sites are given in Table 1.

The representation analysis reveals that, assuming only second-order invariants occur in the spin Hamiltonian, Cu and Nd spins are constrained to lie in the same direction. The absence of a (100) reflection (indexing on the enlarged magnetic cell) and the observation that the calculated magnetic structure factor for (100) is the largest for this configurational spin symmetry imply that spin must lie parallel to the face on which the magnetic structure is centred. The reflection condition $h + k = 2n + 1$ on the magnetic reflections also implies *C*-anticentring. If the cell is *A*-centred then (100) is allowed and (010) is forbidden; hence the magnetic moment $\boldsymbol{m}$ is parallel to (100) as no intensity is observed at this position. The model moments for an *A*-centred structure with Nd and Cu spins parallel to *a* were refined using nonlinear least-squares refinement on the four most intense magnetic peaks uncontaminated by nuclear or λ/2 intensity observed at 1.6 K.† The results of the refinement are shown in Table 2.

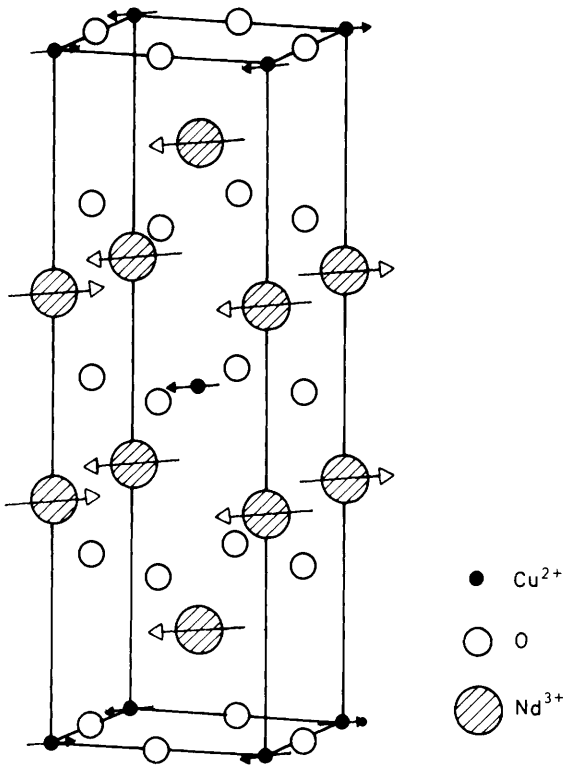

Figure 1. Magnetic structure of Nd_2CuO_4 at 1.6 K.

† The form factor for Cu was obtained by interpolation from the measurements of Freltoft *et al.*[9] and the Nd form factor was calculated in the dipolar approximation from the relativistic calculations of Freeman and Desclaux.[10] The magnetic intensity was scaled to the intensities of the nuclear peaks (002) and (202) and the nuclear structure factors were evaluated from the positional parameters obtained from Rietveld refinements of data obtained on the same samples on the D2B[7] high resolution powder diffractometer.

Table 1. Irreducible representations spanned by moments at Cu [2 at (a) 4/*mmm*] and Nd [4 at (e) 4*mm*] sites in the T′ structure.

Γ_{Cu} =	B_{1g}	B_{2g}	B_{3g}			
Ψ_Γ	m_z	m_y	m_x			
Γ_{Nd} =	B_{1g}	B_{2g}	B_{3g}	A_u	B_{2u}	B_{3u}
Ψ_Γ	$m_z^1 + m_z^2$	$m_y^1 + m_y^2$	$m_x^1 + m_x^2$	$m_z^1 - m_z^2$	$m_x^1 - m_x^2$	$m_y^1 - m_y$

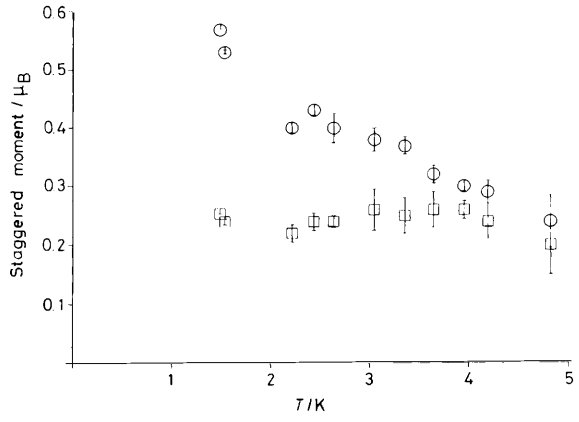

Figure 2. Temperature evolution of Nd and Cu staggered moments for Nd_2CuO_4: ○, Nd; □, Cu.

Table 2. Magnetic structure refinement for B_{3g} modes at Nd and Cu sites in Nd_2CuO_4 and $Nd_{1.97}Ce_{0.03}CuO_4$.

			Nd_2CuO_4			$Nd_{1.97}Ce_{0.03}CuO_4$		
h	*k*	*l*	I_{obs}	ΔI_{obs}	I_{cal}	I_{obs}	ΔI_{obs}	I_{cal}
0	1	1	2.65	0.1	2.65	1.97	0.2	1.97
0	1	3	22.30	0.5	22.25	17.6	1.8	16.6
1	2	0	17.40	0.6	17.52	12.0	1.2	13.1
2	1	3	7.26	0.7	7.15	5.4	1.0	6.3
m_{Cu}/μ_B			0.507(3)			0.45(4)		
m_{Nd}/μ_B			1.136(2)			0.98(2)		
$R_{mag.}^{I}$ [a]/%			0.6			7.9		
χ^2 [b]			1.04			1.02		

[a] $R_{mag}^{I} = 100 \times (I_M^{obs} - I_M^{cal})/I_M^{obs}$. [b] $\chi^2 = 1/(n_{obs} - n_{par}) \times [(I_M^{obs} - I_M^{cal})/\Delta I_{obs}]^2$.

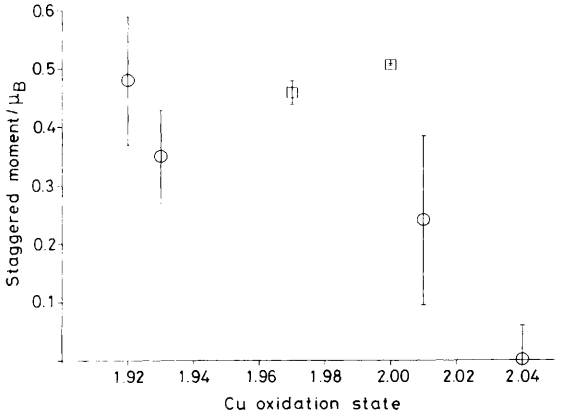

Figure 3. Variation of Cu staggered moment with formal Cu oxidation state in O ($La_{2-x}Sr_xCuO_{4-\delta}$) and T′ ($Nd_{2-x}Ce_xCuO_{4-\delta}$) systems: ○, O structure; □, T′ structure.

The magnetic space group is *C′mm′m′*, *i.e.* the spins lie perpendicular to the unprimed σ_{yz} mirror plane, defined in the $\sqrt{2}a \times \sqrt{2}a \times c$ cell. We may compare the spin structure of the Cu sublattice to La_2NiO_4[11] which also displays a spin direction $(\frac{1}{2},\frac{1}{2},0)$ parallel to the magnetic propagation vector $\boldsymbol{k} = (\frac{1}{2},\frac{1}{2},0)$, and contrast it with that of $La_2CuO_{3.985}$[12] in which the spin direction $(\frac{1}{2}, -\frac{1}{2},0)$ lies perpendicular to the magnetic propagation vector. The magnetic structure is shown in Figure 1. We note, however, that the data do not exclude non-collinear structures. The order of intensity of the other three peaks (104), (124), and (106) is correctly predicted by this model but their intensities are subject to greater error due to subtraction (in view of the existence of Cu order up to high temperatures) and they are not included in the final refinement.

Refinement of the data sets collected up to 5 K shows the staggered moment at the Nd site decreasing with temperature, with the copper moment remaining constant (Figure 2), implying long-range order of the Cu spins above 5 K. A careful examination of the (103) and (101) regions of the pattern revealed weak magnetic intensity at temperatures up to 170 K. It is difficult to extract a reliable T_N from these measurements and to evaluate any change of magnetic structure, but the Cu ordering temperature certainly lies above 160 K. The ordering temperature of the Nd sublattice is higher than in related systems. The coupling between the Nd^{3+} and Cu^{2+} spins, reflected in the moments at both sites transforming according to the same irreducible representation, may be important in explaining the contrast with the behaviour of eight co-ordinate Nd^{3+} in $NdBa_2Cu_3O_{6.85}$, in which the Nd ordering temperature is much lower (551 mK) and the moment is oriented along the *c*-axis,[13] instead of in the basal plane. The observed Nd magnetic moment (1.136 μ_B) is considerably reduced below the free-ion value for Nd^{3+} with a $^4I_{9/2}$ ground multiplet (3.27 μ_B), because of crystal field effects, being consistent with a Kramers ground-state doublet.[14]

Study of the 1.5 K pattern of $Nd_{1.97}Ce_{0.03}CuO_{4-\delta}$ gave the same indexing of the magnetic reflections, and the results of the refinement with the same model used for Nd_2CuO_4 are also included in Table 2. A similar temperature dependence of Nd and Cu staggered moments is also obtained.

The values of the Cu magnetic moment obtained as a function of oxidation state in the T′ structure‡ may be compared with those obtained for the $La_{2-x}Sr_xCuO_{4-\delta}$ system[12,15,16] (which adopts the distorted *Cmca* O structure) (Figure 3). The largest values of the ordered moment display a marked reduction from 1.14 μ_B predicted from $S = \frac{1}{2}$ and $g = 2.28$ for Cu^{2+}. A reduction $\Delta S = 0.18$ is calculated due to zero

‡ Rietveld refinement of the profiles gives $\delta \approx 0$ for $Nd_2CuO_{4-\delta}$ and $\delta \approx 0.02$ for $Nd_{1.97}Ce_{0.03}CuO_{4-\delta}$.

point spin deviations in the 2D Heisenberg model[17] but further reduction of ~15% must be due to covalency. This reflects the decreased transfer integral resulting from the much longer Cu–O bond lengths in the T′ structure, giving a larger localised moment. The surprisingly small difference in moment despite the increased ionic character [1.9585 Å (T′) *vs.* 1.9036 Å (O)[7,16]] may reflect the increased importance of quantum fluctuations in the more 2D T′ structure. Further, the dependence of the ordered moment on doping differs for electron and hole dopings (Figure 3). This may be qualitatively explained in terms of the non-magnetic Cu^{I} states introduced on electron doping, which only affect the onset of magnetic order at the percolation threshold. Assuming that the moment reduction is entirely due to the percolation effect without inclusion of frustration, we find that each Cu^{I} state is delocalised over at least four Cu sites, since 3% doping results in 12% reduction in moment. By contrast, the Cu^{III} states which are introduced on hole doping have a vacant $x^2 - y^2$ level available and a localisation length comparable to the next-nearest-neighbour distances. Thus they can frustrate the magnetic structure by introducing next-nearest-neighbour AF interactions.[16] Alternatively, depending on the relative Cu 3d and O 2p admixture in the σ* band near the Fermi level, the introduction of a p_σ hole on oxygen may also introduce ferromagnetic near-neighbour Cu coupling to frustrate the AF coupling.[2] Hence we expect a much less pronounced effect on the magnetic order of the Cu^{II} background for electrons moving in the upper Hubbard sub-band (T′ structure) than holes moving in the (narrower) lower Hubbard band (O structure). This is entirely consistent with the much higher Ce^{4+} doping levels required for superconductivity[18] and the very narrow range over which it exists since the AF instability must be destroyed before the onset of superconductivity.

In conclusion, we have shown that ordered local magnetic moments appear at the Cu^{2+} sites in both Nd_2CuO_4 (the parent of the electron-doped superconductors) and La_2CuO_4 (the parent of the hole-doped superconductors). Although the magnetic structure is different, they point to the importance of strong correlations in producing superconductivity in cuprates. A Mott–Hubbard description of the strongly correlated σ* electrons in the CuO_2 layers appears appropriate in the T′ as well as the T/O phases. This may be contrasted with the strong electron–phonon coupling $(Ba,K)(Pb,Bi)O_3$ systems where charge-density wave formation is of importance rather than AF correlations. The effect of electron doping is much less marked on the antiferromagnetic structure than hole doping with incommensurate spin density wave behaviour ruled out as the peak positions do not shift with band filling.[16] Nd_2CuO_4 has a relatively high T_N for Nd ordering, pointing to the strong coupling between (Nd_2O_2) and (CuO_2) layers while the Nd spin direction is constrained by symmetry to lie in the same direction as the Cu spin.

We thank the S.E.R.C. for partial support of this work, the Institut Laue-Langevin for provision of neutron time, and J. K. Cockcroft and J.-L. Soubeyroux for help with the diffraction experiments. M. J. R. is a Junior Research Fellow at Merton College and thanks the Leatherseller's Company and St. Catherine's College, Oxford, for a Graduate Scholarship.

Received, 27th July 1989; Com. 9/03197I

References

1 J. G. Bednorz and K. A. Müller, *Z. Phys. B*, 1986, **64**, 189.
2 R. J. Birgeneau, M. A. Kastner, and A. Aharony, *Z. Phys. B*, 1987, **68**, 425.
3 Y. Tokura, H. Takagi, and S. Uchida, *Nature*, 1989, **337**, 345.
4 K. K. Singh, P. Ganguly, and C. N. R. Rao, *Mater. Res. Bull.*, 1982, **17**, 493.
5 G. M. Luke, B. J. Sternlieb, Y. J. Uemura, J. H. Brewer, R. Kadono, R. F. Kiefl, S. R. Kreitzman, T. M. Riseman, J. Gopalakrishnan, A. W. Sleight, M. A. Subramanian, S. Uchida, H. Takagi, and Y. Tokura, *Nature*, 1989, **338**, 49.
6 H. H. Wang, U. Geiser, R. J. Thorn, K. D. Carlson, M. A. Beno, M. R. Monaghan, T. J. Allan, R. B. Proksch, D. L. Stupka, W. K. Kwok, G. W. Crabtree, and J. M. Williams, *Inorg. Chem.*, 1987, **26**, 1190.
7 M. J. Rosseinsky, K. Prassides, and P. Day, *Physica C*, in the press.
8 E. F. Bertaut, *Acta Crystallogr., Sect. A*, 1968, **24**, 217; W. Prandl, 'Topics in Current Physics, Neutron Diffraction,' ed. H. Dachs, Springer Verlag, 1978, ch. 4; A. A. Maradudin and S. H. Vosko, *Rev. Mod. Phys.*, 1968, **40**, 1.
9 T. Freltoft, G. Shirane, S. Mitsuda, J. P. Remeika, and A. S. Cooper, *Phys. Rev. B.*, 1988, **37**, 137.
10 A. J. Freeman and J. P. Desclaux, *J. Magn. Magn. Mater.*, 1979, **12**, 4.
11 G. Aeppli and D. J. Buttrey, *Phys. Rev. Lett.*, 1988, **61**, 203.
12 D. Vaknin, S. K. Sinha, D. E. Moncton, D. C. Johnston, J. Newsam, C. R. Safinya, and H. King, *Phys. Rev. Lett.*, 1987, **58**, 2802.
13 P. Fischer, B. Schmid, P. Brüesch, F. Stucki, and P. Unternährer, *Z. Phys. B*, 1989, **74**, 183.
14 R. Saez-Puche, M. Norton, T. R. White, and W. S. Glaunsinger, *J. Solid State Chem.*, 1983, **50**, 281.
15 R. J. Birgeneau and G. Shirane, 'Physical Properties of High Temperature Superconductors,' ed. D. M. Ginsberg, World Scientific Publishing, 1989.
16 M. J. Rosseinsky, K. Prassides, and P. Day, in preparation.
17 L. J. de Jongh, *Solid State Commun.*, 1988, **65**, 963.
18 H. Takagi, S. Uchida, and Y. Tokura, *Phys. Rev. Lett.*, 1989, **62**, 1197.